Experimental Neurology 322 (2019) 113054

Contents lists available at ScienceDirect

Experimental Neurology

journal homepage: www.elsevier.com/locate/yexnr

Research Paper

Xenon exerts anti-seizure and neuroprotective effects in kainic acid-induced status epilepticus and neonatal hypoxia-induced seizure

Yurong Zhang[a,1], Mengdi Zhang[a,1], Songhua Liu[b], Wei Zhu[c], Jie Yu[a], Yaru Cui[a], Xiaohong Pan[a], Xue Gao[a], Qiaoyun Wang[a], Hongliu Sun[a,*]

[a] School of Pharmaceutical Sciences, Binzhou Medical University, Yantai 264003, China
[b] Clinical Laboratory, Tengzhou Central People's Hospital, Tengzhou, China
[c] Institute of Radiation Medicine, Shandong Academy of Medical Sciences, Jinan 250062, China

ARTICLE INFO

Keywords:
Apoptosis
Neuronal injury
Seizure
Xenon

ABSTRACT

Xenon is an inhalation anesthetic with a favorable safety profile, and previous studies have demonstrated its neuroprotective efficacy. However, whether xenon plays a role in the treatment of epilepsy or seizure remains unclear. This study aimed to investigate the role of xenon inhalation and explore the role of different xenon ratio gradients and different delayed treatment times in seizure models. Kainic acid (KA)-induced status epilepticus and neonatal hypoxia-induced seizure models were used in our study. Animals were subject to inhalation of xenon mixture for 60 min after the stimulation used to induce seizures. The control group was treated with 70% nitrogen/30% oxygen, as in previous reports. Behavioral changes, electroencephalography, neuronal injury, and learning and memory function were investigated in each group. The results indicate that xenon mixture significantly reduced the severity of seizures and neurodegeneration in both KA-induced status epilepticus and in neonatal mice with hypoxia-induced seizure. Moreover, treatment with different percentages of xenon (35%, 50%, or 70%), as well as at different intervention time points (immediately, delayed for 15 min, delayed for 30 min) after hypoxia induction significantly attenuated the severity of seizure and neuronal injury. Additionally, 50% or 70% xenon treatment, as well as immediate xenon treatment or with a delay of 15 min attenuated the learning and memory impairments induced by hypoxia. This study confirmed that xenon mixture exerts strong inhibitive effects in seizure and seizure-induced neuronal injury and defects of cognitive function. Moreover, the results suggest that intervention time window and percentage of xenon influence the efficacy of the xenon treatment. Our study supports that xenon inhalation represents a safe means to inhibit seizures and neuronal injury.

1. Introduction

Epilepsy is a common high-impact disorder with potentially significant long-term consequences. Although several treatment options are currently available for the treatment of epilepsy, current approaches do not fully meet the clinical needs for a safe, effective treatment for epilepsy. Part of the problem arises from the fact that these drugs are typically associated with significant problems such as recrudescence, drug resistance, and significant side effects (Chen et al., 2018; Schmidt and Löscher, 2005). Therefore, developing therapies to attenuate epilepsy or seizure and further reduce neuronal injury and the associated disability is an important clinical priority.

Xenon is a safe anesthetic agent since it lacks toxic side effects and has garnered increasing attention for its neuroprotective effects. In cell culture and animal studies of Alzheimer's disease (AD), xenon has been found to have neuroprotective and restorative effects via the inhibition of glutamate uptake and efflux and furthermore, xenon being reportedly superior to the classic anti-AD drug memantine is of exceptional interest. (Lavaur et al., 2016a,b). In spinal cord ischemia/reperfusion (I/R) injury induced by the ligation of the thoracic aorta, continuous inhalation of xenon for 60 min during reperfusion significantly improves the I/R prognosis, reverses neuronal injury, and reduces neuronal apoptosis (Yang et al., 2012a), even if xenon is inhaled 2 h after reperfusion (Yang et al., 2014). Similar neuroprotective roles were found in rats in which the unilateral common carotid artery was ligated and in mouse models of stroke (Cattano et al., 2011; Metaxa

* Corresponding author.
E-mail address: sun_china6@163.com (H. Sun).
[1] These authors contributed equally to this work.

https://doi.org/10.1016/j.expneurol.2019.113054
Received 11 February 2019; Received in revised form 27 July 2019; Accepted 1 September 2019
Available online 06 September 2019
0014-4886/

et al., 2014). In addition, xenon treatment can reverse neuronal injury and improve cognitive function in a rat model of ischemia and hypoxia induced by intrauterine asphyxia (Yang et al., 2012b).

Significant neuroprotective effects of xenon have been reported for several nervous system diseases, including cerebral ischemia, I/R, spinal cord injury, AD, and so on. In addition, (Uchida et al., 2012) found that xenon treatment could rapidly terminate the neuronal synchronous discharge observed in cultured cortical neurons in vitro. Moreover, it is reported that xenon can reduce the apoptosis induced by overexcitation via inhibition of glutamate uptake and efflux (Lavaur et al., 2016a,b; Preckel et al., 2006; Sinha and Cheung, 2010). As epilepsy is characterized by the synchronous discharge of neurons and neuronal injury, which are closely associated with overexcitation, it is reasonable to speculate that xenon may have anti-epileptic effects.

Although the anti-epileptic efficacy of xenon is theoretically plausible, studies on this topic have been scant. This study aimed to test whether xenon inhalation has anti-seizure and neuroprotective effects in rats with kainic acid (KA)-induced status epilepticus (SE) and neonatal mice with hypoxia-induced seizure. Furthermore, the effective time window of intervention and appropriate percentage range of xenon mixture were explored.

2. Materials and methods

*KA-induced SE*Male Sprague–Dawley rats (240–260 g, Certificate No. SCXK2014–0006; Jinan Jinfeng Experimental Animal Co. Ltd., China) were used. The experiments were conducted in compliance with the ethical guidelines of the Binzhou Medical University Animal Experimentation Committee (approval no. 2016003), Helsinki Declaration of 1975, and the National Institutes of Health *Guide for the Care and Use of Laboratory Animal* (NIH Publications No. 8023, 1978). All efforts were made to minimize the number of animals used and animal suffering. Experimental animals were maintained in individual cages, and water and food were provided ad libitum. All experiments were performed between 9:00 and 17:00 every day.

After anesthesia induction using an intraperitoneal injection of sodium pentobarbital (50 mg/kg, intraperitoneally (i.p.), CAS, 57–33-0, Xiya Reagent, China), rats were fixed in a stereotactic apparatus (Anhui Zheng Hua Biological Instrument Equipment Co., Ltd., China). The tip of twisted-pair stainless steel electrodes (A.M. Systems, USA) was uncoated (0.5 mm), and the electrodes were implanted into the right cortex (anteroposterior, AP: −3.2 mm; mediolateral, ML: −3.0 mm; dorsoventral, DV: −1.8 mm) for electroencephalographic (EEG) recording with a PowerLab device (1–50 Hz, AD Instruments, Australia). EEGs were recorded for 60 min from KA administration to termination by diazepam. The representative EEGs and corresponding frequency-spectrum and power-spectrum density analysis are presented. The stainless-steel cannulas (RSD Life Science, China) were implanted into the right lateral cerebral ventricle (AP: −1.8 mm, ML: −0.96 mm, and DV: −3.8 mm) as previously described (Sun et al., 2018). The animals were allowed to recover from surgery for 7 days.

All rats were treated with KA (1 mg/0.8 ml, 0.65 μl/rat, CAS, 58002–62–3, Sigma, USA), which was injected into the right lateral ventricle through the cannula (Zhang et al., 2019). Immediately after KA administration, signals evincing acute generalized seizures were observed in almost all rats. After 60 min, the seizures were terminated by intraperitoneal injection of diazepam (2 mg/kg).

Seizure severity was staged on a 1–5 scale according to Racine's criteria (Racine, 1972). Cannula placement was histologically verified at the end of the experiment. Only rats with correct implantation in the right lateral cerebral ventricle were counted in the statistical analysis.

2.1. Neonatal hypoxia-induced seizure

C57BL/6 J pregnant mice (Certificate No. SCXK2014-0006; Jinan Jinfeng Experimental Animal Co. Ltd., China) were placed in separate cages and were free to consume sufficient water and food. After birth, 7 days old (P7) young mice were used as experimental subjects. The experiment was conducted between 9:00–17:00. All experiments were in accordance with the National Institutes of Health Laboratory Animal Care and Use Guidelines (NIH Publication No. 8023, revised 1996). The number of animals and the pain experienced by them was minimized. All protocols were approved by the Ethics Committee of Binzhou Medical University (approval no. 2018009). The electrodes were wound on stainless steel screws that were implanted in the skull for EEG recording. The representative EEGs and corresponding frequency-spectrum and power-spectrum density analyses are presented.

P7 C57BL/6J mice in the same litter were used randomly as the hypoxia group and the treatment groups, respectively. We performed the anoxic experiment according to the hypoxic procedure reported in the literature (Jensen et al., 1991; Rakhade et al., 2011).

At first, we prepared the transparent resin observation box with a bottom air inlet and an upper air gate. In the hypoxia group (n = 36), 5% oxygen/95% nitrogen (50 L, Rulin gas Ltd., China) was delivered. The oxygen concentration in the box was checked with the oxygen detector and the temperature was controlled at 34 °C (Rodriguez-Alvarez et al., 2015). Once the oxygen concentration in the chamber reached 5% and remained stable, the 7-day-old mice were placed in the box and treated with 5% oxygen/95% nitrogen for 15 min. EEG recordings in each group were performed for 8 h (9:00–17:00) at different time points (2 h, 24 h, 3 days, 4 weeks, and 2 months after hypoxic treatment). Electroclinical seizure was defined as polyspike discharges > 5 Hz, > 2 times baseline EEG amplitude and longer than 3 s (Rakhade et al., 2011).

2.2. Xenon treatment

In the KA-induced SE model, rats in the xenon group were randomly selected and treated with a xenon mixture (70% xenon/30% oxygen, 50 L, DaTe special gas Ltd., China) for 1 h immediately after KA injection (De Deken et al., 2018) in a transparent resin observation box, which featured a bottom air inlet and an upper air gate. Prior to placing the rats into the box, the 70% xenon mixture was administered for 20 min. The rats in the control group were administered a 70% nitrogen/30% oxygen mixture (50 L, Rulin gas Ltd., China) instead of the xenon mixture (Dingley et al., 2006).

In the hypoxic-induced seizure model, P7 mice were treated with xenon mixture (70% xenon/30% oxygen; 50 L, DaTe special gas Ltd., China) for 1 h at different treatment time points (immediately, 0 min, n = 20; delay of 15 min post-treatment, n = 22; delay of 30 min post-treatment, n = 22) in the a transparent resin observation box, and the mice in the control groups were treated with 30% oxygen/70% nitrogen instead of xenon mixture (Dingley et al., 2006) (n = 20). Furthermore, P7 mice were treated with different percentages of xenon (70% xenon/30% oxygen, 70% xenon group, n = 20; 50% xenon/30% oxygen/20% nitrogen, 50% xenon group , n = 20; or 35% xenon/30% oxygen/35% nitrogen, 35% xenon group, n = 20; 50 L, DaTe special gas Ltd., China) immediately and for 1 h after hypoxia treatment based on previous reports (Arola et al., 2017; De Deken et al., 2018; Liu et al., 2016).

The different gas mixtures were delivered at 200 ml/min via flow regulator valves (DaTe special gas Ltd., China), which were installed in every gas bottle. The EEGs were recorded in each group. The xenon treatment was not enough to induce anesthesia. The rats were kept sober and with free activities during the entire experiment. The temperature of the animals remained stable.

2.3. Morris water maze test

The Morris water maze (ZS-001, Beijing Zhongshi Di Chuang Technology Development Co., Ltd., china) was used to test spatial learning and memory (Morris, 1984). The temperature of the water is optimal at 21–22 °C. The experiment consisted of two parts, the

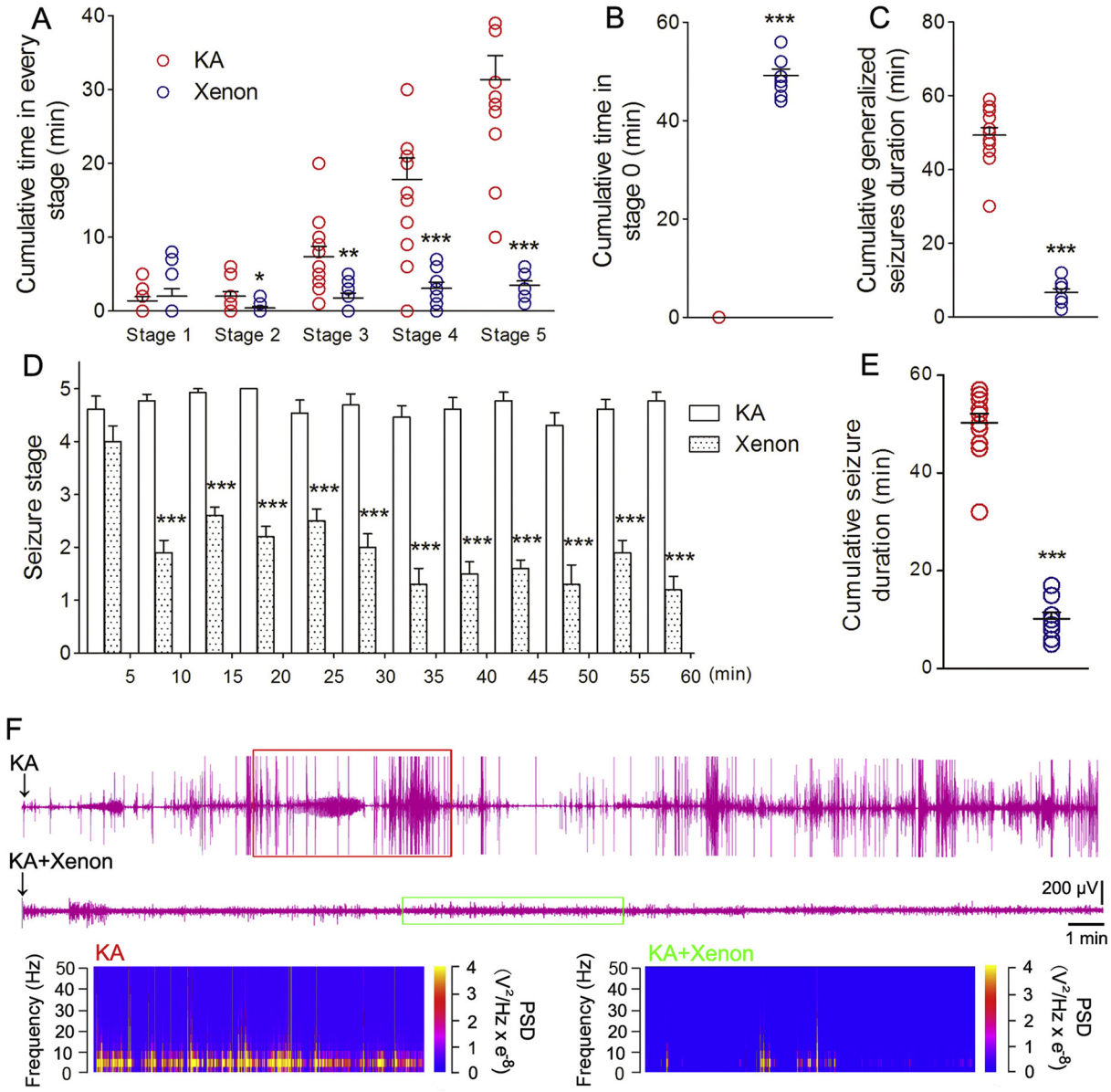

Fig. 1. The therapeutic effects of xenon on acute seizures induced by kainic acid. (A) Cumulative time in every stage. (B) Cumulative time in stage 0. (C) Cumulative generalized seizures duration. (D) Seizure stage in each time period. (E) Cumulative seizure duration. (F) Representative EEGs and power spectrum density analysis of KA group and xenon group. Data are presented as mean ± SEM. Error bars indicate SEM (KA group, $n = 13$; xenon group, $n = 10$; $^{*}P < .05$, $^{**}P < .01$, and $^{***}P < .001$, compared with controls; D, non-parametric Mann-Whitney U test; others, one-way ANOVA).

positioning navigation experiment and the space exploration experiment. The whole experimental process was recorded using a camera above the pool (diameter, 150 cm; height, 50 cm). The positioning navigation test was carried over the first 4 days, allowing the animals to swim freely for 2 min in the pool and become familiar with the surrounding environment. At the beginning of the test, the platform in the 4th transition was 1 cm below the horizontal plane, and the animals were placed in the water from the center of the pool wall from any quadrant of the four quadrants. If the animal did not find the platform within 60 s, the tester used an iron rod to guide the animal to find the platform, without turning the animal's head or body so the animal did not have the illusion of finding the platform with guidance. The animal was then allowed to remain on the platform for 10 s, before being dried and returned to the cage. If the animal did not stay for 10 s and jumped into the water again, the tester again guided it to the platform and permitted it to stay there for 10 s. On the 5th day, a space exploration experiment was carried out. The platform was withdrawn, and the mouse was placed in the water farthest from the platform and allowed to travel for 60 s to search for the platform. Animal spatial learning and memory ability was assessed by the number of times the mouse passed through the platform area , the latency to reach the platform area, the time spent in the target and in the opposite quadrant (Netto et al., 1993; Pereira et al., 2007).

2.4. Western blot analysis

At a designated time point (24 h, or 3 or 7 days after KA administration; or 24 h or 4 weeks following exposure to hypoxia), five rats randomly selected from each group were anesthetized and culled. Brains were immediately removed and the hippocampus, pyriform cortex (PC), and the cortex excluding the PC were microdissected (Sun et al., 2017). After sonication of the tissue, protein content was measured as previously reported (Feng et al., 2016). Equal amounts of protein were loaded and separated using 12% sodium dodecyl sulfate-

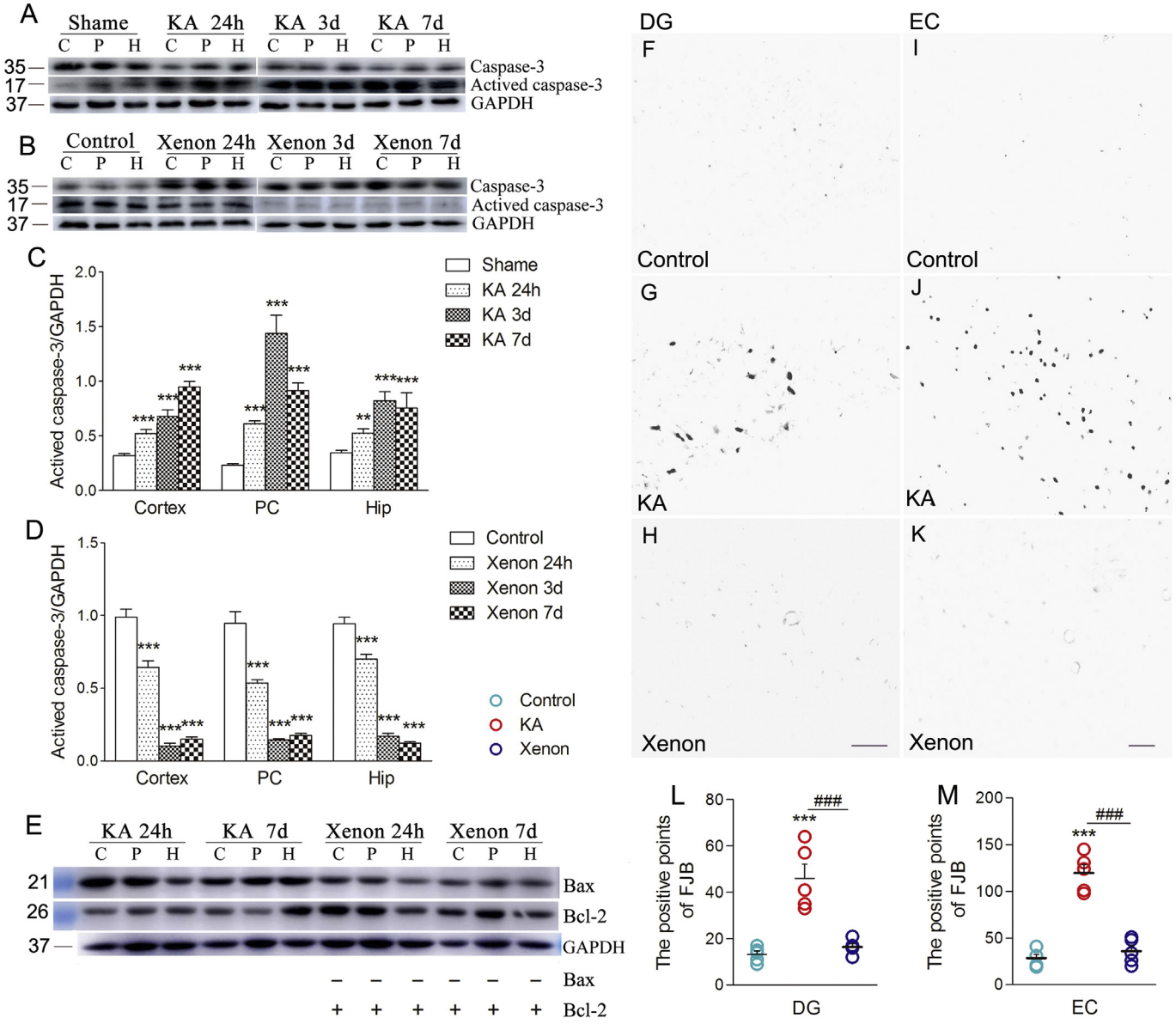

Fig. 2. Xenon treatment attenuated the apoptosis and neuronal injury induced by KA. (A) Immunoreactivity of caspase-3 and activated caspase-3 after KA treatment. (B) Immunoreactivity of caspase-3 and activated caspase-3 after xenon inhalation. (C, D) Normalized intensity of activated caspase-3 relative to GAPDH. (E) Immunoreactivity of Bax and Bcl-2. (F–K) Positive FJB signals in DG and EC in each group (bar = 50 μm). (L, M) Counted positive FJB signals in each group in DG and EC. Data are presented as mean ± SEM. Error bars indicate SEM (n = 5/group; ** P < .01, and ***P < .001, compared with controls; $^{\#\#\#}$P < .001, compared with each other; one-way ANOVA with Dunnett's T3 post-hoc test).

polyacrylamide gels. The protein was then transferred to polyvinylidene difluoride membranes. After blocking with 5% skimmed milk for 1 h, the membranes were then incubated with a mouse monoclonal antibody against B cell lymphoma-2 (Bcl-2, ab32124, 1:1000, Abcam, UK), Bcl-2-associated X protein (Bax, ab77566, 1:1000, Abcam, UK), rabbit monoclonal antibody against activated caspase-3 (ab2302, 1:1000, Abcam, UK), or rabbit polyclonal antibody against caspase-3 (9662, 1:1000, Cell Signaling Technology, USA), or glyceraldehyde-3-phosphate dehydrogenase (GAPDH, AB-P-R 001, 1:2000, Kangchen, China) overnight at 4 °C. Immunoreactive bands were visualized using enhanced chemiluminescence via horseradish peroxidase-conjugated IgG secondary antibodies. The images were acquired with the Odyssey infrared imaging system (LI-COR Biosciences, USA) and analyzed with the accompanying software. The normalized intensity relative to GAPDH was obtained to account for potential differences in initial protein loading.

2.5. Fluoro-Jade B (FJB) staining

FJB is a polyanionic fluorescein derivative, which sensitively and specifically binds to degenerating neurons (Liu et al., 2018). The FJB staining kit (AG310, Millipore, USA) was used in our study. At a designated time point (KA-induced SE rats: 24 h, or 3 or 7 days after KA administration; hypoxic-induced seizure mice: 4 weeks or 2 months after exposure to hypoxia), five rats out of each group were deeply anesthetized and perfused intracardially with normal saline and 4% paraformaldehyde in phosphate-buffered solution. Coronal slices of 10-μm in thickness were made using a cryostat (CM3050s, Leica, Germany). First, the tissue slides were immersed in 80% alcohol solution containing 1% sodium for 5 min. Second, these slides were soaked in 70% alcohol for 2 min and then distilled water for 2 min. Third, in order to ensure the same background between the slides, the slides were immersed a solution containing 0.06% potassium permanganate for 10 min on a rocker; the slides were then rinsed for 2 min with distilled

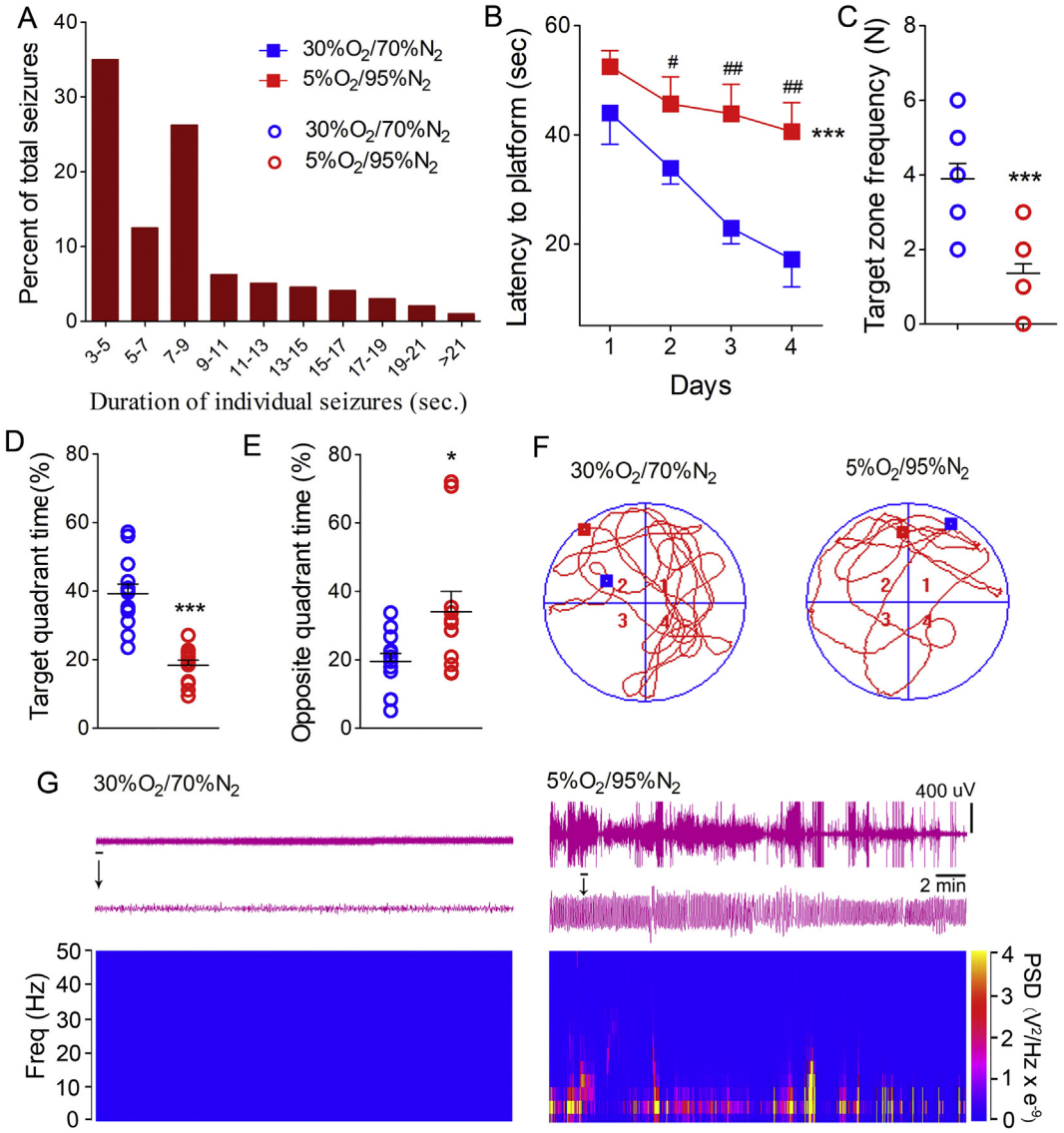

Fig. 3. Hypoxia-induced seizure and decline of learning and memory ability. (A) Percent of total seizures. (B) Latency to the platform (two-way ANOVA). (C) Frequency of platform crossings. (D) Target quadrant time (%). (E) Opposite quadrant time (%). (F) Representative tracking. (G) Representative EEGs and power spectrum density. Data are presented as mean ± SEM. Error bars indicate SEM. *P < .05, ***P < .001, compared with controls, #P < .05 and ##P < .01, compared with controls every day, one-way ANOVA with Dunnett's T3 post-hoc test.

water. Dye powder was used to make a 0.01% FJB stock solution composed of 96 ml 0.1% acetic acid vehicle and 4 ml FJB stock solution to make a 100 ml staining solution. The staining solution was prepared within 10 min. The slides were soaked in the staining solution for 20 min and were rinsed for 1 min with distilled water. After rinsing, the slides were placed in an oven set at 50 °C for 5 min. Finally, the dry slides were immersed in xylene for 1 min. The slides were mounted with neutral balsam and then observed under a non-fluorescent microscope (Rodriguez-Alvarez et al., 2015). Positive signals were counted manually.

2.6. Statistical analysis

All data were collected in a blinded manner. Data are presented as mean ± standard error of the mean (SEM). Statistical analysis was conducted using SPSS version 13.0 (SPSS Inc., Chicago, IL, USA) for Windows. After normal distribution tests were performed, one-way analysis of variance followed by a Dunnett's T3 post-hoc test was conducted for the multiple comparisons of cumulative seizure duration, generalized seizures duration (GSD), number of seizure frequency, target zone frequency, protein expression levels, and positive signals in FJB staining. Latency to platform was analyzed by two-way ANOVA for repeated measures. The non-parametric Mann-Whitney *U* test was used to analyze the seizure stage in each time period. For all analyses, a two-tailed *P*-value of < 0.05 was considered to be the threshold for statistical significance.

3. Results

3.1. Xenon treatment attenuated the KA-induced acute seizures

In the KA group (n = 13), the rats underwent exposure to the 70% nitrogen/30% oxygen mixture immediately after KA administration. In our study, almost all of the rats entered the state of generalized seizures immediately without intervention after KA administration. Moreover, the intermittent SE was observed in the 60 min prior to termination using diazepam. Thus, we analyzed the differences among the generalized seizures in every group. The amount of time the rats spent at

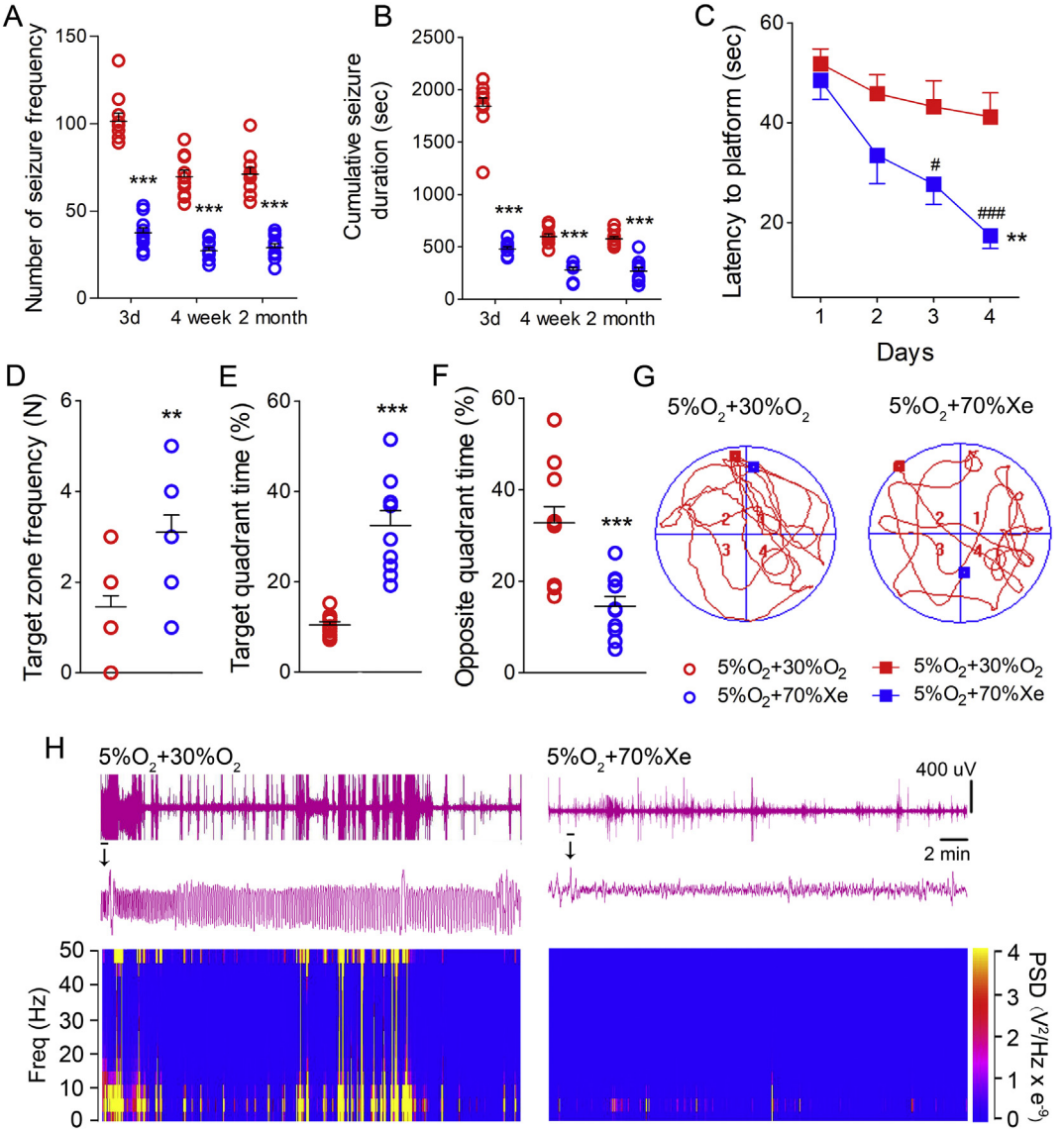

Fig. 4. Xenon treatment attenuated the seizure and decline of learning and memory induced by hypoxia. (A) Cumulative number of seizures. (B) Cumulative seizure duration. (C) Latency to the platform (two-way ANOVA). (D) Frequency of platform crossings. (E) Target quadrant time (%). (F) Opposite quadrant time (%). (G) Representative tracking. (H) Representative EEGs and power spectrum density. Data are presented as mean ± SEM. Error bars indicate SEM. **P < .01 and ***P < .001, compared with controls; #P < .05 and ###P < .001, compared with controls every day, one-way ANOVA with Dunnett's T3 post-hoc test.

stages 5 and 4 was approximately 31.4 ± 3.2 min and 17.8 ± 2.9 min, respectively (Fig. 1A). The accumulated time in the generalized seizure state was 49.2 ± 2.1 min (Fig. 1A). In the xenon group (n = 10), the 70% xenon/30% oxygen mixture was inhaled immediately after KA administration. Compared with the rats in the KA group, the behavioral stage of the rats in the xenon group was significantly lower than that in the KA group (Fig. 1A). The accumulated times spent in stages 4 and 5 were only approximately 3.1 ± 0.9 min and 3.5 ± 1.1 min, respectively, and the duration was significantly shorter in the xenon than in the KA group (P < .001 and 0.001, respectively; Fig. 1A). Moreover, the rats in the xenon group spent approximately 49.2 ± 1.3 min in stage 0 (no seizure stage), while rats in the KA group were continuously in different seizure stages for 60 min, from KA administration to diazepam-induced termination of the seizures (P < .001, Fig. 1B). During these 60 min, the accumulated GSD in the xenon group was significantly shorter than that in the KA group (6.6 ± 2.1 min and 49.2 ± 2.1 min, respectively; P < .001; Fig. 1C). A similar decrease was found for seizure duration measures (10.2 ± 1.3 min and 50.2 ± 1.8 min, respectively; P < .001; Fig. 1E) based on the EEG analysis. Moreover, mortality in the xenon treatment group was 0, while 3 out of 13 rats died in the KA group. These results indicate that xenon treatment significantly attenuated the severity of seizure.

The differences in the seizure stages were further compared every 5 min in the xenon and control groups to characterize the onset time of the therapeutic effect of xenon. The results show that from the second 5-min period of measurement, the seizure intensity in the xenon group was already significantly weaker than that in the control group (stage 1.9 ± 0.2 and stage 4.8 ± 0.1, respectively; P < .001; Fig. 1D). These results indicate that during acute seizures, the therapeutic effect of xenon was observed as early as 5–10 min. Fig. 1F shows the representative EEGs and corresponding frequency spectrum and power spectrum density in each group.

3.2. Xenon treatment reduced the apoptosis and neurodegeneration induced by KA

Changes in apoptotic markers were investigated in the xenon-treated group and non-xenon-treated group (n = 5 per group). Changes

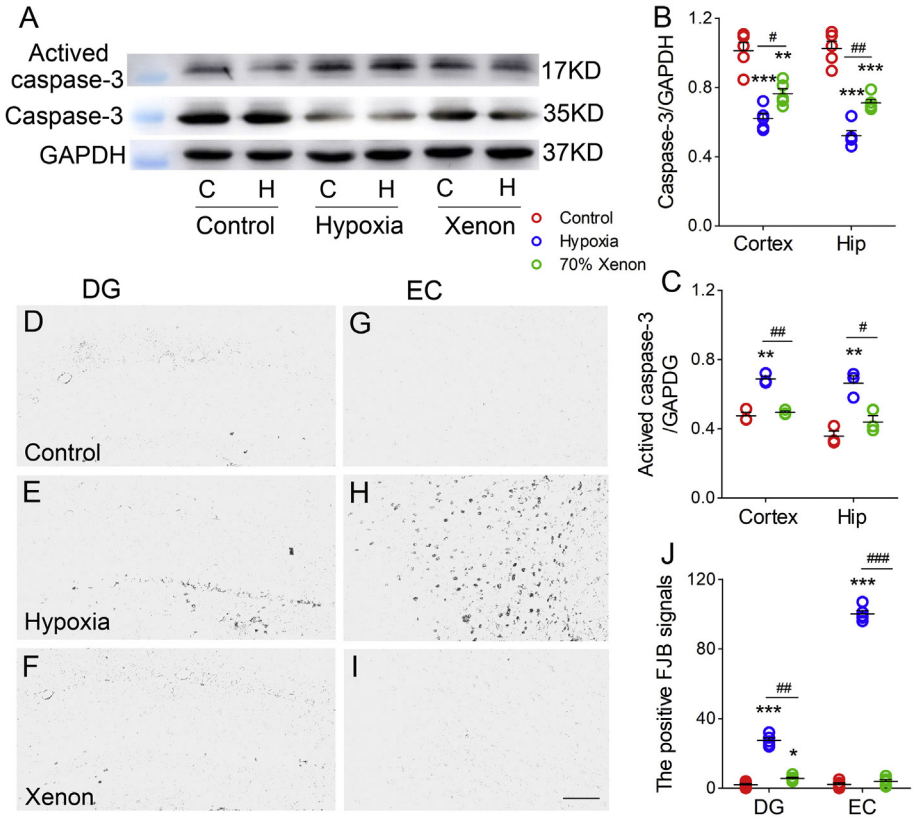

Fig. 5. Xenon treatment attenuated apoptosis and neuronal injury induced by hypoxia. (A) Immunoreactivity of caspase-3 and activated caspase-3 after hypoxia treatment. (B, C) Normalized intensity of caspase-3 and activated caspase-3 relative to GAPDH. (D–I) Positive FJB signals in DG and EC on 4th week in each group (bar = 50 μm). (J) Counted positive FJB signals in each group in DG and EC. Data are presented as mean ± SEM. Error bars indicate SEM (n = 5/group; *P < .05, **P < .01, and ***P < .001, compared with controls; #P < .05, ##P < .01 and ###P < .001, compared with each other; one-way ANOVA with Dunnett's T3 post-hoc test).

in caspase-3, activated caspase-3 (apoptosis marker), Bax (promoter of apoptosis), and Bcl-2 (inhibitor of apoptosis) were analyzed. In the KA group, activated caspase-3 significantly increased in the PC ($P < .001$, Fig. 2A, C), cortex other than the PC (P < .001, Fig. 2A, C), and in the hippocampus ($P = .004$, Fig. 2A, C) 24 h after KA administration. Xenon treatment prevented the increase in activated caspase-3 (P < .001, Fig. 2B, D) induced by KA administration. A decrease in Bax expression and an increase in Bcl-2 expression were observed in the xenon group, when compared with the control group treated only with KA (Fig. 2E). Therefore, xenon treatment could prevent the increase in apoptosis induced by KA administration.

FJB staining was performed in every group (n = 5/group) to assess neurodegeneration after KA administration. The results showed that KA administration increased the positive signals of FJB staining in hippocampus and cortex relative to those of the controls treated with saline from 24 h following KA administration. The significant increase in FJB signals on the 3rd day are shown (dentate gyrus (DG), $P < .001$, Fig. 2G, L; entorhinal cortex (EC), P < .001, Fig. 2J, M). The increase in positive signals induced by KA was reversed by 70% xenon mixture inhalation ($P < .001$, Fig. 2H, K, L, and M). The FJB staining results indicate that neurodegeneration occurred in the KA-induced status epilepticus (SE) model and 70% xenon mixture inhalation could significantly attenuate this change.

3.3. Xenon treatment attenuated the hypoxia-induced seizure and defects in learning and memory

The effects of xenon mixture were assessed in the neonatal mice with hypoxia-induced seizure. After the 15 min hypoxia treatment, the P7 neonatal C57 mice were immediately subjected to the 70% xenon mixture. Seizures were recorded at designated time points. The hypoxia treatment significantly induced seizure in the P7 C57 mice (Fig. 3A). The representative EEGs and power spectrum analysis are presented in Fig. 3G. Moreover, learning and memory ability was assessed in each group on the 6th week. The longer latency to the platform (P < .001, Fig. 3B), fewer crossings ($P < .001$, Fig. 3C) in the platform, the shorter time in target quadrant (P < .001, Fig. 3D) and the longer time in opposite quadrant ($P = .024$, Fig. 3E) which indicate defects in learning and memory, were observed in the mice exposed to hypoxia.

The xenon treatment significantly reduced the severity of hypoxia-induced seizure, such as the number of seizure frequency ($P < .001$, Fig. 4A) and cumulative seizure duration (P < .001, Fig. 4B) in mice treated with 30% O_2/70% xenon than in those treated with 30% O_2/70% N_2 after hypoxia. Moreover, the latency to the platform was shorter ($P = .001$, Fig. 4C) and the frequency of platform crossings was larger ($P = .002$, Fig. 4D), accompanied with longer time in target quadrant (P < .001, Fig. 4E) and shorter time in opposite quadrant (P < .001, Fig. 4F) in the mice treated with the xenon mixture. The representative tracking of each group in the Morris water maze test is shown in Fig. 3G.

3.4. Xenon treatment attenuated the apoptosis and neuronal injury induced by hypoxia in C57 mice

Changes in apoptosis and neuronal injury were assessed in the 70% xenon-treated group compared with the non-xenon-treated group in hypoxia-induced seizure C57 mice. The results indicate that the immunoreactivity of activated caspase-3 was remarkably elevated 24 h after hypoxia treatment (cortex, $P = .001$, Fig. 5A, C; hippocampus, $P = .004$, Fig. 5A, C). Inhalation of 70% xenon inhalation significantly attenuated the level of caspase-3 activation in the xenon-treated group compared with the increased level in the hypoxia exposed group (cortex, P = .001; hippocampus, $P = .016$; Fig. 5A, C). Furthermore, the neurodegeneration in each group was assessed by FJB staining on the 4th week. The results showed that the positive FJB signals were significantly increased after hypoxia treatment in the DG ($P < .001$, Fig. 5E, J) and EC (P < .001, Fig. 5H, J). Moreover, the increased positive signals were significantly reduced in the group treated with

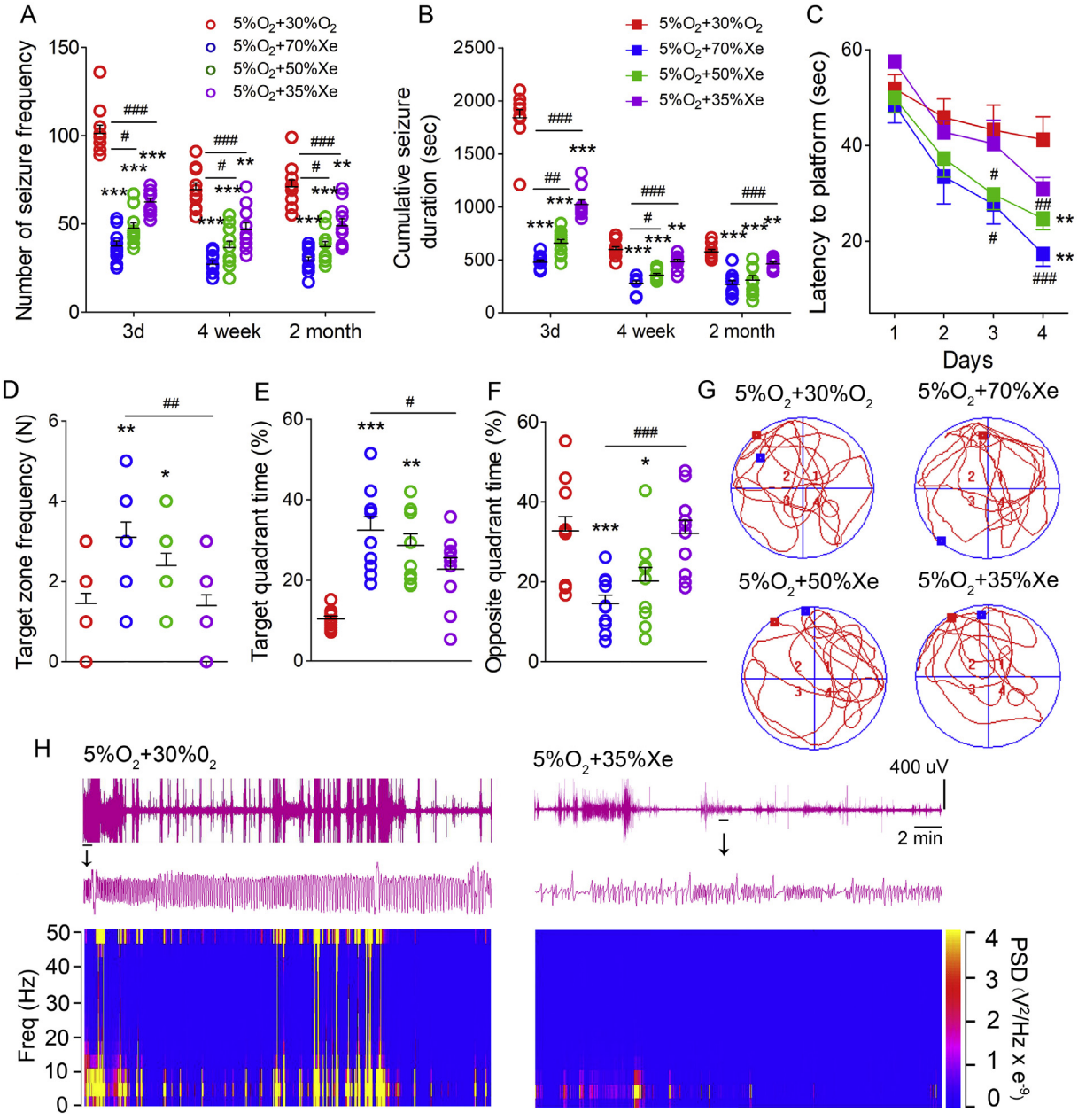

Fig. 6. Effect of different percentages of xenon mixture on hypoxia-induced seizure in C57 mice. (A) Number of seizure frequency. (B) Cumulative seizure duration. (C) Latency to the platform (two-way ANOVA). (D) Frequency of platform crossings. (E) Target quadrant time (%). (F) Opposite quadrant time (%). (G) Representative tracking. (H) Representative EEGs and power spectrum density. Data are presented as mean ± SEM. Error bars indicate SEM. *P < .05, **P < .01 and ***P < .001, compared with controls; #P < .05, ##P < .01 and ###P < .001, compared with each other; one-way ANOVA with Dunnett's T3 post-hoc test.

xenon mixture immediately after 15 min hypoxia treatment (DG, $P = .008$; EC, P < .001; Fig. 5F, I and J). The immunoreactivity for activated caspase-3 detected by western blot and positive signals by FJB staining confirmed that hypoxia induced apoptosis and neuronal injury and that treatment with xenon could significantly attenuate this.

3.5. Effects of different percentages of xenon mixture on hypoxia-induced seizure in C57 mice

P7 C57 mice were treated with different percentages of xenon mixture (35%, 50% and 70%) immediately after exposure to hypoxia. Seizure severity was assessed by counting the number of seizures frequency and cumulative seizure duration in each group. The results show that all percentages of xenon could significantly reduce the number of seizures frequency at the time points investigated (3 days, 4 weeks, 2 months; Fig. 6A) and the cumulative seizure duration (Fig. 6B). The more effective anti-seizure effects were provided by 70% xenon treatment (Fig. 6A, B). The representative EEGs and power spectrum density analysis are shown in Fig. 6H.

The Morris water maze experiment explored the difference in learning and memory ability in each group. The results show that the latency to the platform was significantly reduced in groups treated with 50% ($P = .001$) or 70% (P = .001) xenon and no effect was found in the group treated with 35% xenon ($P = .361$) (Fig. 6C). Similarly, more frequent platform crossings (50%, $P = .025$; 70%, $P = .002$), longer time in target quadrant (50%, P = .002; 70%, $P < .001$) and shorter time in the opposite quadrant (50%, $P = .016$; 70%, P < .001) were found in the groups treated with 50% or 70% xenon, but not in the group treated with 35% xenon (Fig. 6D–F). A representative track of the mice searching for the platform in each group is shown in Fig. 6G. The

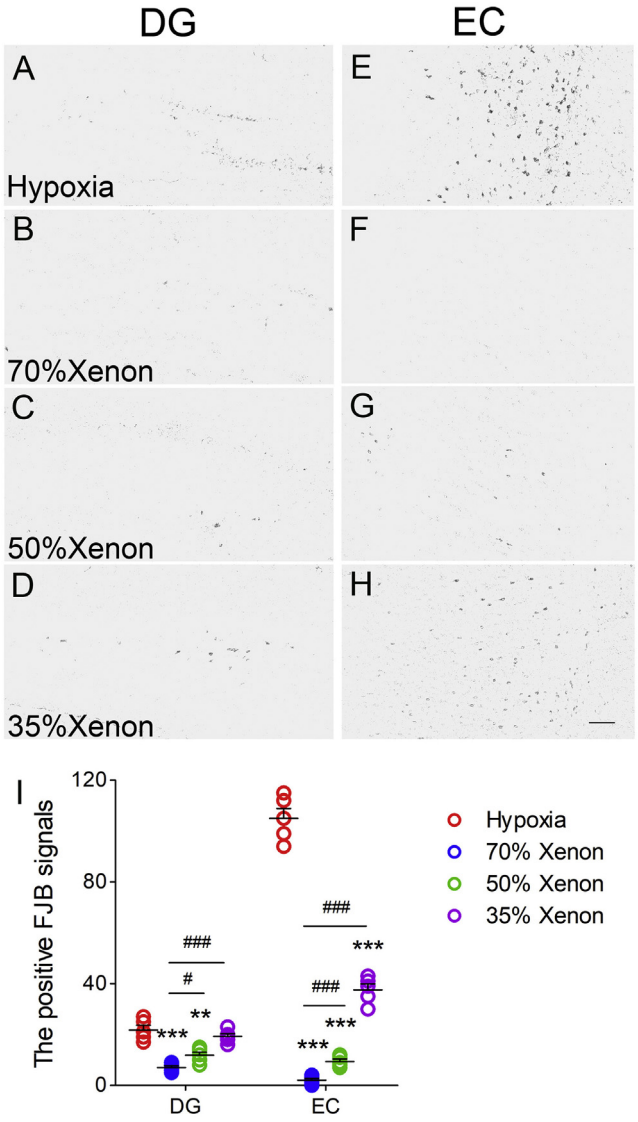

Fig. 7. Effect of different percentages of xenon treatment on apoptosis and neuronal injury induced by hypoxia. (A–H) Positive FJB signals in DG and EC on 4th week in each group (bar = 50 μm). (I) Counted positive FJB signals in each group in DG and EC. Data are presented as mean ± SEM. Error bars indicate SEM (n = 5/group; **P < .01, and ***P < .001, compared with controls; #P < .05, ###P < .001, compared with each other; one-way ANOVA with Dunnett's T3 post-hoc test).

results indicate that 35%, 50%, or 70% xenon treatment could attenuate the severity of seizure, and 50% or 70% xenon treatment could attenuate the reduction in learning and memory ability induced by hypoxia.

Neuronal injury was assessed by FJB staining in each group in the 4th week. The results show that all xenon mixtures (35%, 50%, or 70%) could attenuate the positive FJB signals in the EC (Fig. 7F–I) and PC (data not shown). Additionally, 50% or 70% xenon treatment could attenuate the FJB signals in the DG (Fig. 7B, C, I). The results confirmed the anti-seizure effects and neuronal protection provided by 35%, 50%, and 70% xenon mixtures.

3.6. Effects of different intervention time points of xenon mixture on hypoxia-induced seizure in C57 mice

Different time delays (delay of 15 min or 30 min) prior to xenon intervention were used following hypoxia treatment in P7 C57 mice to mimic the inevitable delay before therapeutic intervention in the clinic. Both the number of seizures frequency and cumulative seizure duration were significantly reduced in mice treated with xenon with different periods of delay (delay of 0 min, delay of 15 min, or delay of 30 min; Fig. 8A and B). Representative EEGs and power spectrum density analysis results are shown in Fig. 8H. Analysis of learning and memory ability showed that xenon was effective with a delay of 0 min (Latency to the platform, P = .001, Fig. 8C; frequency of platform crossings, P = .002; Fig. 8D; target quadrant time, P < .001, Fig. 8E; opposite quadrant time, P < .001, Fig. 8F), or a delay of 15 min (Latency to the platform, *P* = .022, Fig. 8C; frequency of platform crossings, *P* = .029, Fig. 8D; target quadrant time, *P* = .003, Fig. 8E; opposite quadrant time, P = .016, Fig. 8F), but no effect was found in the group that had a delay of 30 min (Latency to the platform, *P* = .241, Fig. 8C; frequency of platform crossings, *P* = .693, Fig. 8D; target quadrant time, *P* = .509, Fig. 8E; opposite quadrant time, *P* = .902, Fig. 8F). The representative tracking for the platform in each group is presented in Fig. 8G.

FJB staining results indicate that the positive signals were significantly reduced in mice treated with xenon with a delay of 30 min (Fig. 9A–I). The detected effective time window of xenon intervention supports the feasibility of using xenon treatment for anti-seizure effects and neuronal protection.

4. Discussion

Although previous reports strongly suggest a possible anti-epileptic effect of xenon, the role of xenon in seizures remains unclear. The current study aimed to assess the role of xenon in preventing seizure and neuronal injury. We found that inhalation of a specific xenon mixture (70% xenon/30% oxygen) strongly inhibited the acute generalized seizure induced by KA administration, leading to reduced apoptosis and neurodegeneration. The protective effects of xenon mixture were verified in C57 neonatal mice, including attenuated seizure severity, reduced apoptosis, reduced neuronal injury, and reduced learning and memory defects. Furthermore, the percentage range from 35% to 70% was confirmed as being effective and the 70% xenon mixture provided the most significant effects in mice with hypoxia-induced seizure. Additionally, the protective effects of 70% xenon were verified up to a treatment delay of 30 min in neonatal mice with hypoxia-induced seizure.

Further studies were performed to investigate the role of xenon inhalation in preventing apoptosis and neuronal injury. Epileptic seizure is a disorder associated with neuronal overexcitation. The accumulation of glutamate in the brain, resulting in excitotoxicity, is a critical factor in the occurrence and propagation of epilepsy (During and Spencer, 1993; Luna-Munguia et al., 2019). Excessive accumulation of extracellular glutamate over-activates *N*-methyl-D-aspartate (NMDA) and α-amino-3-hydroxy-5-methyl-4-isoxazolepropionic acid receptors, among others. Excessive excitation of the NMDA receptor leads to the occurrence of acute nerve injury, such as neuronal dysfunction and apoptosis, by activating calpain and the caspase-3 pathway (Baudry and Bi, 2016; Izumida et al., 2017; Hoque et al., 2016). Apoptosis and nerve loss are important pathological changes in both patients and animal models of epilepsy (Jafarian et al., 2018; Liang et al., 2016). Xenon treatment has been reported to inhibit the uptake and efflux of glutamate (Lavaur et al., 2016a), further upregulating the anti-apoptotic protein Bcl-2 and downregulating the apoptosis promoting protein Bax. Ultimately, these effects may underlie its neuroprotective effect through the inhibition of excessive excitation and by promoting anti-apoptotic effects (Preckel et al., 2006; Sinha and Cheung, 2010). We therefore investigated the influence of xenon in apoptosis and neuronal injury in KA-induced acute generalized seizures and hypoxia-induced seizures. Our results indicate that, consistent with its inhibitive effect on seizure, xenon significantly inhibited apoptosis and neurodegeneration in both KA-induced SE rats and mice with hypoxia-induced

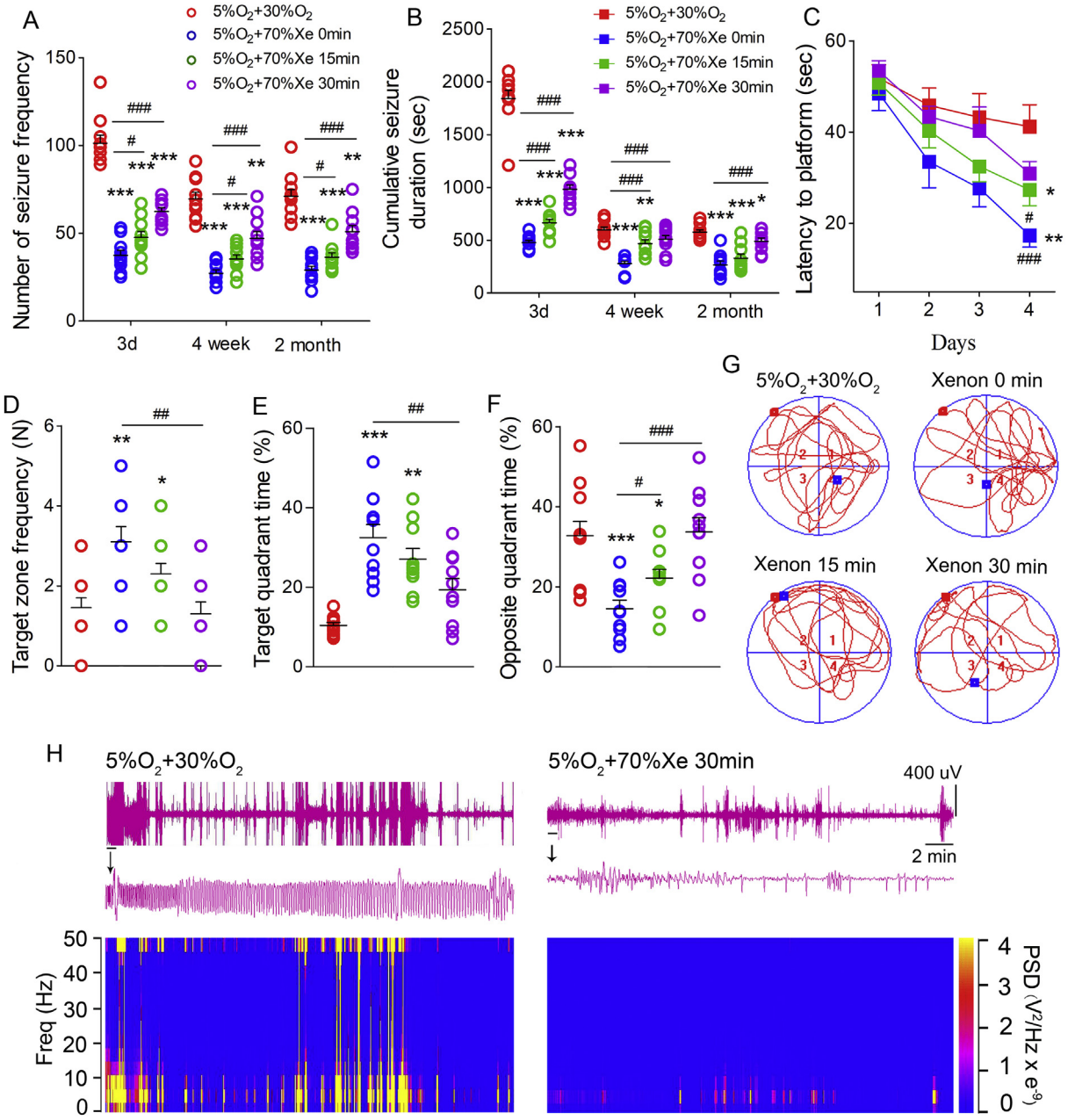

Fig. 8. Effect of different delay time points for xenon mixture treatment on hypoxia-induced seizure in C57 mice. (A) Number of seizure frequency. (B) Cumulative seizure duration. (C) Latency to the platform (two-way ANOVA). (D) Frequency of platform crossings. (E) Target quadrant time (%). (F) Opposite quadrant time (%). (G) Representative tracking. (H) Representative EEGs and power spectrum density. Data are presented as mean ± SEM. Error bars indicate SEM. *P < .05, **P < .01 and ***P < .001, compared with controls; #P < .05, ##P < .01 and ###P < .001, compared with each other; one-way ANOVA with Dunnett's T3 post-hoc test.

seizure.

As an inert gas, xenon is characterized as having non-toxic effects and a high level of safety. Moreover, our study confirmed the anti-seizure and neuroprotective roles of xenon mixture at a subanesthetic level. The rats are sober and have free movement during the xenon treatment. Xenon mixture treatment may be a convenient, feasible, and safe intervention for terminating seizure and inducing neuroprotection. It is necessary to confirm the effective percentage gradient and treatment time point of xenon mixture for its proper use as a clinical therapy.

Neonatal hypoxia is one important type of perinatal hypoxia that is highly likely to cause epilepsy in newborns (Zhou et al., 2011). The studies indicate that neonatal epilepsy or seizure can directly lead to brain injury (Dzhala et al., 2000; Glass et al., 2009; Hall et al., 1998). Moreover, some hypoxia-induced seizures are resistant to existing anti-convulsant drugs (Sanchez, 2005). Additionally, anti-convulsant drugs may be partly responsible for injury during brain development in newborns (Olney et al., 2014; Sankar and Rho, 2007). The reduction in seizure and neuronal injury observed following xenon treatment suggests that xenon may yield therapeutic prospects for neonatal hypoxia.

Neonatal mice with hypoxia-induced seizure were treated with different percentages of xenon mixture immediately after hypoxia. Significant anti-seizure and neuroprotective effects were found in all xenon treated groups (35%, 50%, and 70% xenon mixture) and the best effects were provided by 70% xenon mixture. The results indicate that once effective percentages of xenon have been established, along with the time period within which treatment must occur, xenon could significantly attenuate hypoxia-induced seizure, neuronal injury, and

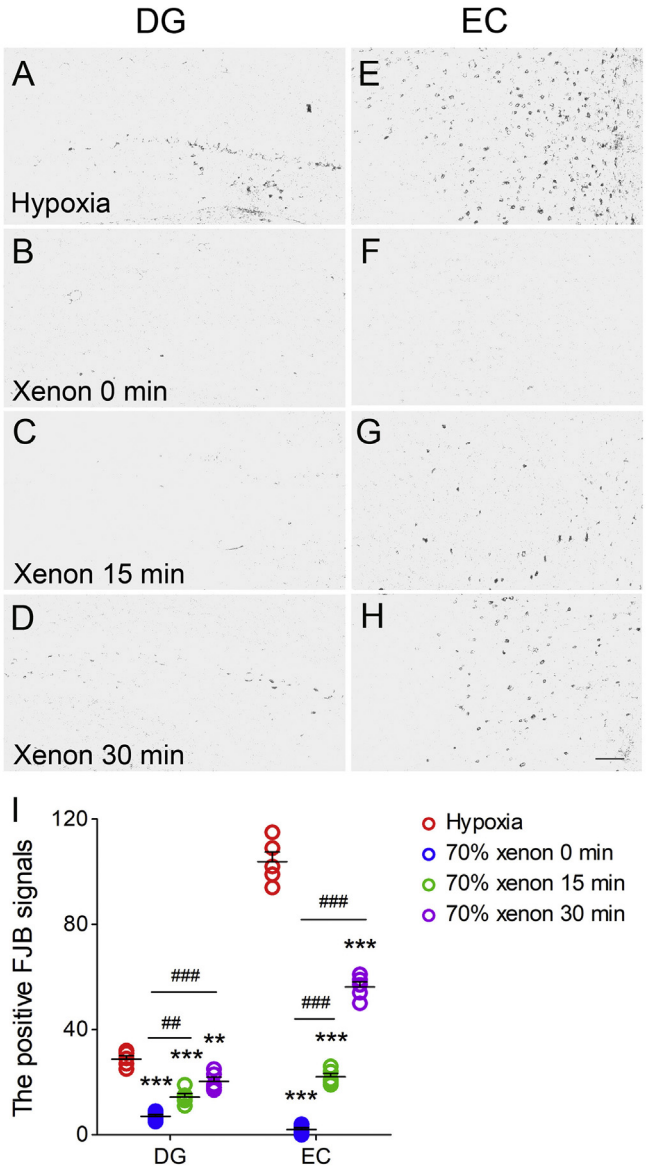

Fig. 9. Effect of different percentages of xenon treatment on apoptosis and neuronal injury induced by hypoxia. (A–H) Positive FJB signals in DG and EC on 4th week in each group (bar = 50 μm). (I) Counted positive FJB signals in each group in DG and EC. Data are presented as mean ± SEM. Error bars indicate SEM (n = 5/group; **P < .01 and ***P < .001, compared with controls; ##P < .01 and ###P < .001, compared with each other; one-way ANOVA with Dunnett's T3 post-hoc test).

defects in learning and memory.

Considering the possible delay in the time from hypoxia exposure to clinical therapy, it is necessary to evaluate the time frame within which xenon is effective in future studies. Significant effects of xenon treatment were found in the group treated with xenon immediately and the groups treated after a delay (delay of 15 min and delay of 30 min). The results indicate the feasibility of using xenon treatment as a therapeutic option for neonatal hypoxia.

Neonatal hypoxia has serious consequences (Dzhala et al., 2000; Glass et al., 2009; Hall et al., 1998; Zhou et al., 2011), and drug treatments are inadequate (Olney et al., 2014; Sanchez, 2005; Sankar and Rho, 2007). As previously mentioned, xenon has been characterized as being non-toxic and safe. Thus, if one or several short-term treatments with xenon can produce significant anti-seizure and neuroprotective effects, xenon may have good clinical prospects.

In this study, neurodegeneration was evaluated by FJB staining. The results confirmed neuronal injury in the hippocampus (especially DG and CA3 subregions), EC, and PC in seizure models. These subregions are vital in the epileptic network, as well as in cognitive function (Hsu, 2007; Xu et al., 2010). The hippocampus-EC cycle is known as a vital regulator for cognitive function and epileptic synchronized activity, and EC is involved in the initiation of hippocampal information input (Basu et al., 2016; Buzsáki and Moser, 2013; Hafting et al., 2005). In this network, the hippocampus was considered the primary promoter and amplifier region (Heinemann et al., 1992; Hsu, 2007) for epileptic activity in both longitudinal (Derchansky et al., 2006) and contralateral (Blackstad, 1956) propagation. The interictal 0.5–1 Hz discharge in the CA3 subregion of the hippocampus prevents both the inputted epileptiform activity initiated from the EC and further propagation to the CA1-subiculum network (Barbarosie and Avoli, 1997). Additionally, the EC is confirmed as a gate to the hippocampus, and prominent suppression in the EC has been verified during seizure development (Gnatkovsky et al., 2008). Moreover, mimicking the interictal-like discharges in hippocampal-EC slices could inhibit epileptogenesis (Xu et al., 2010). The PC is closely connected with the ipsilateral hippocampus, EC, and amygdala (Löscher and Ebert, 1996), and the contralateral amygdala and PC through the anterior commissure (Schwabe et al., 2004), and was considered to participate in the development and generalization of epilepsy (Zhu-Ge et al., 2007).

Our FJB staining results indicate that neurodegeneration of the hippocampus, EC, and PC may play a role in seizure and the cognitive deficits. Neuronal injury in the hippocampus, EC, and PC may be responsible for defects in effective control of depressed networks. Attenuation of neuronal injury in these subregions by treatment with an appropriate xenon mixture may represent the mechanism underlying its protective effects.

5. Conclusions

In summary, our study provides evidence to support the strong therapeutic effect of xenon treatment in KA-induced SE and hypoxia-induced seizure. Moreover, we optimized the effective percentage gradient and time window for treatment with xenon mixture. Given the lack of toxic side effects, the inhalation of xenon may be an effective and safe new strategy for the treatment of seizure.

Author contributions

YR Z and MD Z: study conception and design, data acquisition. SH L, W Z and J Y: KA-induced rat model preparation, data acquisition, data analysis and interpretation. YR C, XH P, X G, and QY W: data acquisition and data analysis. HL S: study design, data acquisition and drafting of manuscript.

Declaration of Competing Interest

None.

Acknowledgements

This project was supported by grants from the National Science Foundation of China (81573412), Key Research and Development Plan (2018GSF121004), and Natural Science Foundation (ZR2014JL055, ZR2015HL040) of Shandong Province. We would like to thank Editage for English language editing.

References

Arola, O., Saraste, A., Laitio, R., Airaksinen, J., Hynninen, M., Bäcklund, M., et al., 2017. Inhaled xenon attenuates myocardial damage in comatose survivors of out-of-hospital cardiac arrest: the xe-hypotheca trial. J. Am. Coll. Cardiol. 70, 2652–2660. https://

doi.org/10.1016/j.jacc.2017.09.1088.
Barbarosie, M., Avoli, M., 1997. CA3-driven hippocampal-entorhinal loop controls rather than sustains in vitro limbic seizures. J. Neurosci. 17, 9308–9314. https://doi.org/10.1523/JNEUROSCI.17-23-09308.1997.
Basu, J., Zaremba, J.D., Cheung, S.K., Hitti, F.L., Zemelman, B.V., Losonczy, A., et al., 2016. Gating of hippocampal activity, plasticity, and memory by entorhinal cortex long-range inhibition. Science 351 (6269), 138–154. https://doi.org/10.1126/science.aaa5694.
Baudry, M., Bi, X., 2016. Calpain-1 and Calpain-2: the yin and yang of synaptic plasticity and neurodegeneration. Trends Neurosci. 39, 235–245. https://doi.org/10.1016/j.tins.2016.01.007.
Blackstad, T.W., 1956. Commissural connections of the hippocampal region in the rat, with special reference to their mode of termination. J. Comp. Neurol. 105, 417–537. https://doi.org/10.1002/cne.901050305.
Buzsáki, G., Moser, E.I., 2013. Memory, navigation and theta rhythm in the hippocampal-entorhinal system. Nat. Neurosci. 16 (2), 130–138. https://doi.org/10.1038/nn.3304.
Cattano, D., Valleggi, S., Cavazzana, A.O., Patel, C.B., Ma, D., Giunta, F., 2011. Xenon exposure in the neonatal rat brain: effects on genes that regulate apoptosis. Minerva Anestesiol. 77, 571–578.
Chen, Z., Brodie, M.J., Liew, D., Kwan, P., 2018. Treatment outcomes in patients with newly diagnosed epilepsy treated with established and new antiepileptic drugs: a 30-year longitudinal cohort study. JAMA Neurol. 75 (3), 279–286. https://doi.org/10.1001/jamaneurol.2017.3949.
De Deken, J., Rex, S., Lerut, E., Martinet, W., Monbaliu, D., Pirenne, J., et al., 2018. Postconditioning effects of argon or xenon on early graft function in a porcine model of kidney autotransplantation. Br. J. Surg. 105, 1051–1060. https://doi.org/10.1002/bjs.10796.
Derchansky, M., Rokni, D., Rick, I.J., Wennberg, R., Bardakjian, B.L., Zhang, L., et al., 2006. Bidirectional multisite seizure propagation in the intact isolated hippocampus: the multifocality of the seizure “focus”. Neurobiol. Dis. 23, 312–328. https://doi.org/10.1016/j.nbd.2006.03.014.
Dingley, J., Tooley, J., Porter, H., Thoresen, M., 2006. Xenon provides short-term neuroprotection in neonatal rats when administered after hypoxia-ischemia. Stroke. 37 (2), 501–506. https://doi.org/10.1161/01.STR.0000198867.31134.ac.
During, M.J., Spencer, D.D., 1993. Extracellular hippocampal glutamate and spontaneous seizure in the conscious human brain. Lancet 341, 1607–1610. https://doi.org/10.1016/0140-6736(93)90754-5.
Dzhala, V., Ben-Ari, Y., Roustem Khazipov, M.D., 2000. Seizures accelerate anoxia-induced neuronal death in the neonatal rat hippocampus. Ann. Neurol. 48 (4), 632. https://doi.org/10.1002/1531-8249(200010)48:4<632::AID-ANA10>3.0.CO;2-3.
Feng, B., Tang, Y., Chen, B., Xu, C., Wang, Y., Dai, Y., et al., 2016. Transient increase of interleukin-1β after prolonged febrile seizures promotes adult epileptogenesis through long-lasting upregulating endocannabinoid signaling. Sci. Rep. 6, 21931. https://doi.org/10.1038/srep21931.
Glass, H.C., Glidden, D., Jeremy, R.J., Barkovich, A.J., Ferriero, D.M., Miller, S.P., 2009. Clinical neonatal seizures are independently associated with outcome in infants at risk for hypoxic–ischemic brain injury. J. Pediatr. 155, 318–323. https://doi.org/10.1016/j.jpeds.2009.03.040.
Gnatkovsky, V., Librizzi, L., Trombin, F., de Curtis, M., 2008. Fast activity at seizure onset is mediated by inhibitory circuits in the entorhinal cortex in vitro. Ann. Neurol. 64 (6), 674–686. https://doi.org/10.1002/ana.21519.
Hafting, T., Fyhn, M., Molden, S., Moser, M.B., Moser, E.I., 2005. Microstructure of a spatial map in the entorhinal cortex. Nature 436 (7052), 801–806. https://doi.org/10.1038/nature03721.
Hall, R.T., Hall, F.K., Daily, D.K., 1998. High-dose phenobarbital therapy in term newborn infants with severe perinatal asphyxia: a randomized, prospective study with three-year follow-up. J. Pediatr. 132, 345–348. https://doi.org/10.1016/S0022-3476(98)70458-5.
Heinemann, U., Beck, H., Dreier, J.P., Ficker, E., Stabel, J., Zhang, C.L., 1992. The dentate gyrus as a regulated gate for the propagation of epileptiform activity. Epilepsy Res. Suppl. 7, 273–280. https://doi.org/10.1111/j.1528-1157.1992.tb05897.x.
Hoque, A., Hossain, M.I., Ameen, S.S., Ang, C.S., Williamson, N., Ng, D.C., et al., 2016. A beacon of hope in stroke therapy- blockade of pathologically activated cellular events in excitotoxic neuronal death as potential neuroprotective strategies. Pharmacol. Ther. 160, 159–179. https://doi.org/10.1016/j.pharmthera.2016.02.009.
Hsu, D., 2007. The dentate gyrus as a filter or gate: a look back and a look ahead. Prog. Brain Res. 163, 601–613. https://doi.org/10.1016/S0079-6123(07)63032-5.
Izumida, H., Takagi, H., Fujisawa, H., Iwata, N., Nakashima, K., Takeuchi, S., et al., 2017. NMDA receptor antagonist prevents cell death in the hippocampal dentate gyrus induced by hyponatremia accompanying adrenal insufficiency in rats. Exp. Neurol. 287, 65–74. https://doi.org/10.1016/j.expneurol.2016.08.007.
Jafarian, M., Modarres Mousavi, S.M., Alipour, F., Aligholi, H., Noorbakhsh, F., Ghadipasha, M., et al., 2018. Cell injury and receptor expression in the epileptic human amygdala. Neurobiol. Dis. 124, 416–427. https://doi.org/10.1016/j.nbd.2018.12.017.
Jensen, F.E., Applegate, C.D., Holtzman, D., Belin, T.R., Burchfiel, J.L., 1991. Epileptogenic effect of hypoxia in the immature rodent brain. Ann. Neurol. 29, 629–637. https://doi.org/10.1002/ana.410290610.
Lavaur, J., Lemaire, M., Pype, J., Le Nogue, D., Hirsch, E.C., Michel, P.P., 2016a. Neuroprotective and neurorestorative potential of xenon. Cell Death Dis. 7, e2182. https://doi.org/10.1038/cddis.2016.86.
Lavaur, J., Lemaire, M., Pype, J., Le Nogue, D., Hirsch, E.C., Michel, P.P., 2016b. Xenon-mediated neuroprotection in response to sustained, low-level excitotoxic stress. Cell Death Dis. 2, 16018. https://doi.org/10.1038/cddiscovery.2016.18.
Liang, S., Zhang, L., Yu, X., Zhang, S., Zhang, G., Ding, P., 2016. Neuroprotective effect of electric conduction treatment on hippocampus cell apoptosis in KA induced acute temporal lobe epileptic rats. Brain Stimul. 9, 933–939. https://doi.org/10.1016/j.brs.2016.07.011.
Liu, S., Yang, Y., Jin, M., Hou, S., Dong, X., Lu, J., et al., 2016. Xenon-delayed post-conditioning attenuates spinal cord ischemia/reperfusion injury through activation AKT and ERK signaling pathways in rats. J. Neurol. Sci. 368, 277–284. https://doi.org/10.1016/j.jns.2016.07.009.
Liu, T., Ma, X., Ouyang, T., Chen, H., Xiao, Y., Huang, Y., et al., 2018. Efficacy of 5-aminolevulinic acid-based photodynamic therapy against keloid compromised by downregulation of SIRT1-SIRT3-SOD2-mROS dependent autophagy pathway. Redox Biol. 17, 195–203. https://doi.org/10.1016/j.redox.2018.10.011.
Löscher, W., Ebert, U., 1996. The role of the piriform cortex in kindling. Prog. Neurobiol. 50, 427–481. https://doi.org/10.1016/S0301-0082(96)00036-6.
Luna-Munguia, H., Zestos, A.G., Gliske, S.V., Kennedy, R.T., Stacey, W.C., 2019. Chemical biomarkers of epileptogenesis and ictogenesis in experimental epilepsy. Neurobiol. Dis. 121, 177–186. https://doi.org/10.1016/j.nbd.2018.10.005.
Metaxa, V., Lagoudaki, R., Meditskou, S., Thomareis, O., Oikonomou, L., Sakadamis, A., 2014. Delayed post-ischaemic administration of xenon reduces brain damage in a rat model of global ischaemia. Brain Inj. 28, 349–364. https://doi.org/10.3109/02699052.2013.865273.
Morris, R., 1984. Developments of a water-maze procedure for studying spatial learning in the rat. J. Neurosci. Methods 11 (1), 47–60. https://doi.org/10.1016/0165-0270(84)90007-4.
Netto, C.A., Hodges, H., Sinden, J.D., Le Peillet, E., Kershaw, T., Sowinski, P., et al., 1993. Effects of fetal hippocampal field grafts on ischaemic-induced deficits in spatial navigation in the water maze. Neuroscience 54 (1), 69–92. https://doi.org/10.1016/0306-4522(93)90384-R.
Olney, J.W., Young, C., Wozniak, D.F., Jevtovic-Todorovic, V., Ikonomidou, C., 2014. Do pediatric drugs cause developing neurons to commit suicide? Trends Pharmacol. Sci. 25 (3), 135–139. https://doi.org/10.1016/j.tips.2004.01.002.
Pereira, L.O., Arteni, N.S., Petersen, R.C., da Rocha, A.P., Achaval, M., Netto, C.A., 2007. Effects of daily environmental enrichment on memory deficits and brain injury following neonatal hypoxia–ischemia in the rat. Neurobiol. Learn. Mem. 87, 101–108. https://doi.org/10.1016/j.nlm.2006.07.003.
Preckel, B., Weber, N.C., Sanders, R.D., Maze, M., Schlack, W., 2006. Molecular mechanisms transducing the anesthetic, analgesic, and organ-protective actions of xenon. Anesthesiology. 105, 187–197.
Racine, R.J., 1972. Modification of seizure activity by electrical stimulation: II Motor seizure. Electroencephalogr. Clin. Neurophysiol. 32, 281–294. https://doi.org/10.1016/0013-4694(72)90177-0.
Rakhade, S.N., Klein, P.M., Huynh, T., Hilario-Gomez, C., Kosaras, B., Rotenberg, A., et al., 2011. Development of later life spontaneous seizures in a rodent model of hypoxia-induced neonatal seizures. Epilepsia. 52 (4), 753–765. https://doi.org/10.1111/j.1528-1167.2011. 02992.x.
Rodriguez-Alvarez, N., Jimenez-Mateos, E.M., Dunleavy, M., Waddington, J.L., Boylan, G.B., Henshall, D.C., 2015. Effects of hypoxia-induced neonatal seizures on acute hippocampal injury and later-life seizure susceptibility and anxiety-related behavior in mice. Neurobiol. Dis. 83, 100–114. https://doi.org/10.1016/j.nbd.2015.08.023.
Sanchez, R.M., 2005. AMPA/Kainate Receptor-mediated downregulation of GABAergic synaptic transmission by calcineurin after seizures in the developing rat brain. J. Neurosci. 25 (13), 3442–3451. https://doi.org/10.1523/JNEUROSCI.0204-05.2005.
Sankar, R., Rho, J.M., 2007. Do seizures affect the developing brain? Lessons from the laboratory. J. Child Neurol. 22 (5 Suppl). https://doi.org/10.1177/0883073807303072. (21S-9S).
Schmidt, D., Löscher, W., 2005. Drug resistance in epilepsy: putative neurobiologic and clinical mechanisms. Epilepsia. 46 (6), 858–877. https://doi.org/10.1111/j.1528-1167.2005.54904.x.
Schwabe, K., Ebert, U., Löscher, W., 2004. The central piriform cortex: anatomical connections and anticonvulsant effect of GABA elevation in the kindling model. Neuroscience 126, 727–741. https://doi.org/10.1016/j.neuroscience.2004.04.022.
Sinha, A.C., Cheung, A.T., 2010. Spinal cord protection and thoracic aortic surgery. Curr. Opin. Anaesthesiol. 23, 95–102. https://doi.org/10.1097/ACO.0b013e3283348975.
Sun, H.L., Zhu, W., Zhang, Y.R., Pan, X.H., Zhang, J.R., Chen, X.M., et al., 2017. Altered glutamate metabolism contributes to antiepileptogenic effects in the progression from focal seizure to generalized seizure by low-frequency stimulation in the ventral hippocampus. Epilepsy Behav. 68, 1–7. https://doi.org/10.1016/j.yebeh.2016.09.009.
Sun, H.L., Ma, L.Y., Zhang, Y.R., Pan, X.H., Wang, C.Y., Zhang, J.J., et al., 2018. A purinergic P2 receptor family-mediated increase in thrombospondin-1 bolsters synaptic density and epileptic seizure activity in the amygdala-kindling rat model. Front. Cell. Neurosci. 12, 302. https://doi.org/10.3389/fncel.2018.00302.
Uchida, T., Suzuki, S., Hirano, Y., Ito, D., Nagayama, M., Gohara, K., 2012. Xenon-induced inhibition of synchronized bursts in a rat cortical neuronal network. Neuroscience. 214, 149–158. https://doi.org/10.1016/j.neuroscience.2012.03.063.
Xu, Z.H., Wu, D.C., Fang, Q., Zhong, K., Wang, S., Sun, H.L., et al., 2010. Therapeutic time window of low-frequency stimulation at entorhinal cortex for amygdaloid-kindling seizures in rats. Epilepsia. 51 (9), 1861–1864. https://doi.org/10.1111/j.1528- 1167.2010.02663.x.
Yang, Y.W., Lu, J.K., Qing, E.M., Dong, X.H., Wang, C.B., Zhang, J., et al., 2012a. Post-conditioning by xenon reduces ischaemia- reperfusion injury of the spinal cord in rats. Acta Anaesthesiol. Scand. 56, 1325–1331. https://doi.org/10.1111/j.1399-6576. 2012.02718.x.
Yang, T., Zhuang, L., Rei Fidalgo, A.M., Petrides, E., Terrando, N., Wu, X., et al., 2012b. Xenon and sevofluranne provide analgesia during labor and fetal brain protection in a perinatal rat model of hypoxia-ischemia. PLoS One 7, e37020. https://doi.org/10.1371/journal.pone.0037020.

Yang, Y.W., Cheng, W.P., Lu, J.K., Dong, X.H., Wang, C.B., Zhang, J., et al., 2014. Timing of xenon-induced delayed postconditioning to protect against spinal cord ischaemia-reperfusion injury in rats. Br. J. Anaesth. 117, 168–176. https://doi.org/10.1093/bja/aet352.

Zhang, Y.R., Zhu, W., Yu, H.Y., Yu, J., Zhang, M.D., Pan, X.H., et al., 2019. P2Y4/TSP-1/TGF-β1/pSmad2/3 pathway contributes to acute generalized seizures induced by kainic acid. Brain Res. Bull. 149, 106–119. https://doi.org/10.1016/j.brainresbull.2019.04.004.

Zhou, C., Lippman, J.J., Sun, H., Jensen, F.E., 2011. Hypoxia-induced neonatal seizures diminish silent synapses and long-term potentiation in hippocampal CA1 neurons. J. Neurosci. 31 (50), 18211–18222. https://doi.org/10.1523/JNEUROSCI.4838-11.2011.

Zhu-Ge, Z.B., Zhu, Y.Y., Wu, D.C., Wang, S., Liu, L.Y., Hu, W.W., et al., 2007. Unilateral low-frequency stimulation of central piriform cortex inhibits amygdaloid-kindled seizures in Sprague-Dawley rats. Neuroscience 146 (3), 901–906. https://doi.org/10.1016/j.neuroscience.2007.02.014.